지진응답자료를 사용한 화련 지반-구조물 상호작용계의 지진입력운동과 지반계수의 추정

Input and System Identification of the Hualien Soil-Structure Interaction System Using Earthquake Response Data

최준성*　　이종세**

Choi, Junseong*　　Lee, Jongseh**

국문요약

본 논문에서는 지반-구조물 상호작용계의 입력하중과 강성에 관련된 물성값들을 구조물에서 계측된 지진응답만을 사용하여 효과적으로 추정할 수 있는 새로운 방법을 제안하였는데, 제안된 방법은 미지계수 추정을 위한 목적함수가 입력하중에 독립적이기 때문에 구조물에서 계측된 지진응답만으로 미지계수의 추정이 가능하도록 되어 있다. 본 연구에서 제안된 방법의 검증은 국제공동 연구의 일환으로 최근 대만의 화련에 건설된 대형지진시험 구조물에서 계측된 지진 응답을 사용하여 수행하였다. 추정된 입력하중과 지반과 구조물의 강성에 관련된 물성값들을 사용하여 계산된 지진응답이 계측치와 매우 잘 일치하여, 추정결과의 타당성을 검증할 수 있었다.

1. Introduction

Many techniques have been proposed to develop analytical models correlated with experimental data to study soil-structure interaction (SSI). These techniques generally work well for the cases where numerical simulation data or experimental data are obtained from small structural models. However, most of the techniques appear to be erratic for large-scale soil-structure interaction systems, due to the nonlinear behaviors of the near field soil media and the radiation damping [1,2]. Besides, these techniques need also to overcome problems associated with the uncertainty of the input motion in the earthquake response analysis. Therefore, it is desired that a new method be developed so that an analytical model can be correlated with the test data regardless of the input motion. To that end, a new method is proposed in this study by combining the optimization technique and the input identification technique thereby enabling estimation of the input motion as well as the system properties using the response data only. The proposed method is applied to the Hualien large-scale seismic test structure. The parameters identified are the input motion as well as the shear moduli of the near-field soil

* 한양대학교 토목환경공학과 BK21 연구교수
** 한양대학교 토목환경공학과 교수

regions and Young's moduli of the shell sections of the structure. The earthquake response analysis on the soil-structure interaction system is carried out using the finite element method combined with the infinite element formulation for the unbounded layered soil medium and the substructured wave input technique [3]. The constrained steepest descent method is employed to obtain the revised parameters. Then parameters are identified for the NS-direction based on the earthquake response data and compared with those from the forced vibration test data and input motion measured at the free-field of the Hualien site. The simulated earthquake responses using the identified parameters and the input motion show excellent agreement with the observed response data.

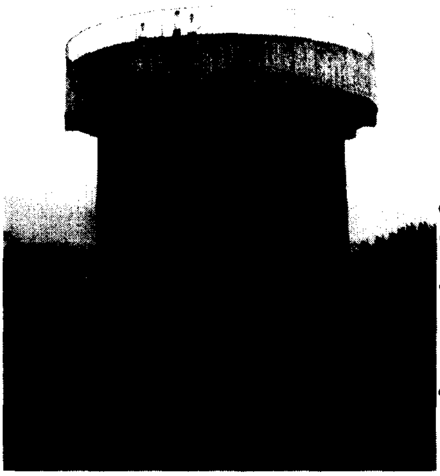

Figure 1 Hualen LSST structure

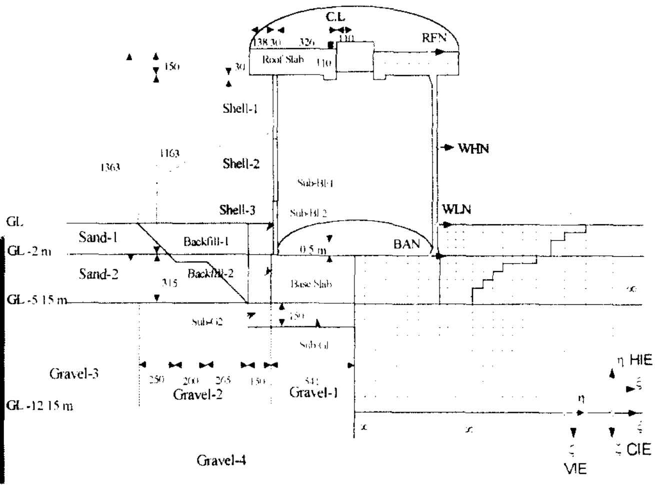

Figure 2 Modeling of the Hualien soil-structure system

2. Unified Model

For a benchmark comparison of the various SSI analysis techniques proposed by the consortium members [1], a unified soil model was constructed using the data from the geological exploration and in-situ tests carried out by CRIEPI of Japan [4]. The stiffness properties of the containment structure were evaluated from the design drawings and the values recommended by Taiwan Power Company (TPC) [2]. The parameters of the unified model are shown in Table 1.

3. Finite-Infinite Element Earthquake Response Analysis

The soil-structure interaction is a very complicated phenomenon requiring an analytical model with a certain level of sophistication for a meaningful earthquake response analysis. In particular, frequency-dependent characteristics and the effect of radiation damping due to the unbounded nature of far-field soil medium should at least be incorporated. To that end, the axisymmetric finite-infinite element model used in the FVT correlation analysis is utilized in this study. The infinite elements have nodes only along the interface between the near and the far field regions (Γ_i) as shown in Figure 2.

Table 1. Properties of soil-structure system for the unified and updated models

Soil and Structure Region	Stiffness Property*			Poisson's Ratios	Mass Density (kg/m^3)	Damping Ratio (h)
	Unified Model	FVT-Correlated [2]	This Study			
Backfill-1	400	270	273	0.38	2330	0.02
Backfill-2	400	325	309	0.48	2390	0.02
Sand-1	133	133	128	0.38	1690	0.02
Sand-2	231	231	226	0.48	1930	0.02
Gravel-1	383	308	309	0.48	2420	0.02
Gravel-2	333	281	267	0.47	2420	0.02
Gravel-3	476	388	392	0.47	2420	0.02
(Shell-1)		19.7	19.3			
Shell (Shell-2)	28.2	21.3	19.9	0.167	2570	0.02
(Shell-3)		21.8	21.5			
Roof & Base Slabs	28.2	28.2	28.2	0.167	2570	0.02

* Shear wave velocities for soil medium are in *m/sec*, and Young's moduli for structure are in *GPa*.

Based on the rigid-exterior boundary method [5], earthquake responses can be computed by solving the following wave radiation equation

$$\begin{bmatrix} \mathbf{S}_{nn}(\omega) & \mathbf{S}_{ni}(\omega) \\ \mathbf{S}_{in}(\omega) & \mathbf{S}_{ii}(\omega)+\widetilde{\mathbf{S}}_{ii}(\omega) \end{bmatrix} \begin{Bmatrix} \mathbf{u}_n(\omega) \\ \mathbf{u}_i(\omega) \end{Bmatrix} = \begin{Bmatrix} \mathbf{0} \\ \mathbf{f}_i(\omega) \end{Bmatrix} \tag{1}$$

in which $\mathbf{u}(\omega)$ is the total displacement vector with respect to a fix point in space; $\mathbf{S}(\omega)$ is the dynamic stiffness matrix obtained by the finite element formulation for the near field; $\widetilde{\mathbf{S}}(\omega)$ is the dynamic stiffness matrix computed by the infinite element formulation for the far field region; and $\mathbf{f}_i(\omega)$ is the equivalent earthquake force along the interface (Γ_i) as shown in Figure 2, which can be calculated from the free-field responses as

$$\mathbf{p}_i^f(\omega) = \widetilde{\mathbf{S}}_{ii}(\omega)\mathbf{u}_i^f(\omega) - \mathbf{A}\mathbf{t}_i^f(\omega) \tag{2}$$

where $\mathbf{u}_i^f$ and $\mathbf{t}_i^f$ are the displacement and the traction on Γ_i obtained from the free-field analysis and $\mathbf{A}$ is a constant transformation matrix. The dynamic stiffness matrix of the far-field, $\widetilde{\mathbf{S}}_{ii}(\omega)$, can be computed by assembling the element matrices of the infinite elements as

$$\widetilde{\mathbf{S}}^{(e)}(\omega) = (1 + j2h^{(e)})\widetilde{\mathbf{K}}^{(e)}(\omega) - \omega^2\widetilde{\mathbf{M}}^{(e)}(\omega) \tag{3}$$

where $j=\sqrt{-1}$; $h^{(e)}$ is the hysteretic damping ratio of infinite element (e); and $\widetilde{\mathbf{K}}^{(e)}(\omega)$ and $\widetilde{\mathbf{M}}^{(e)}(\omega)$ are the element stiffness and mass matrices, respectively [6].

4. Preliminary Investigation

Preliminary investigations for the sake of domain identification related to a finite element analysis are made on the soil properties obtained from the geological exploration, results from a static stress analysis for the subsoil layers during various construction stages, and the predicted earthquake responses using the unified soil model. The results of the preliminary investigations are summarized as the following :

Table 2 Upper and lower bounds

Partitioned Regions	Lower Bounds*	Upper Bounds*
Backfill-1 Backfill-2	190	400
Sand-1	100	133
Sand-2	180	231
Gravel-1	280	383
Gravel-2	255	333
Gravel-4	333	476
Shell Structure	18.3	28.2

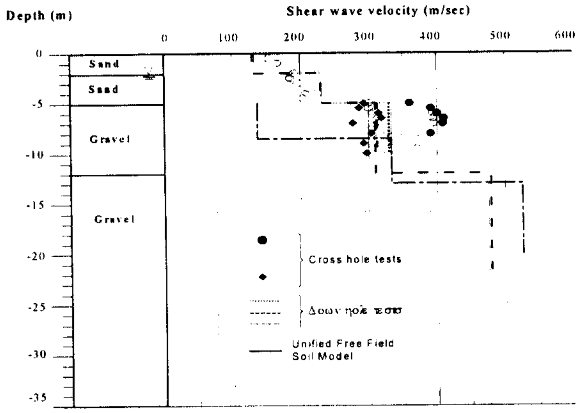

Figure 3 Soil profile of the Hualien test site [4]

(1) Comparisons of the predicted earthquake responses using the unified model with the measured data indicate that the stiffness properties of the unified soil model are generally overly stiff [2]. Therefore, the upper bounds of the shear moduli of the soil media are taken as those of the unified model, while the lower bounds are determined from the geological test data as shown in Figure 3.

(2) From a static analysis, it is found that the shear moduli of Gravel-1 and Sand-2 shall be greater than those of Gravel-2 and Sand-1, respectively. The shear modulus of Gravel 3 region is taken to be greater than that of Gravel 1 based on the free field soil profile in Figure 3.

(3) The backfill soil region is divided into two layers with different properties, namely, Backfill-1 and Backfill-2, since the region near the ground surface is physically separated by ground water table and has a critical influence upon responses of the structure. Based on the results of the static analysis, the shear modulus of Backfill-2 is taken to be greater than that of Backfill-1.

(4) It was speculated that the stiffness of the shell section of the structure, particularly in the upper part, may be weakened due to the temporary openings in the shell during the construction period [2]. Based on the above observation, the spatial variation of the shell stiffness along the height is represented by introducing three uniform regions as in Figure 2, while the stiffness of the roof slab and the foundation is taken as the value of the unified model.

Consequently, ten regions are selected for identification of the stiffness parameters, which include Shell-1, Shell-2, Shell-3, Sand-1, Sand-2, Backfill-1, Backfill-2, Gravel-1, Gravel-2, and Gravel-3 as shown in Figure 2. The lower and upper bounds of the stiffness properties are summarized in Table 2.

5. Formulation of Parameter Identification

The shear and Young's moduli of the ten regions are updated to correlate the FE models with the earthquake response data. The parameters are represented by the base values $\overline{G}_r$, which are taken as those of the unified model, and the correction parameters p_r to be identified as:

$$G_r = \overline{G}_r(1+p_r) \quad \text{and} \quad |\,p_r\,| < 1 \quad (r = 1,2,\cdots,N_p) \tag{4}$$

where N_p is the number of parameters, i.e. $N_p = 10$ in this study. Thus we can express the estimated frequency response function $\mathbf{H}(\mathbf{p},\omega_s)$ of the soil-structure system under the earthquake excitation with a circular frequency of ω_s in terms of the stiffness parameters $\mathbf{p}$ as:

$$\mathbf{H}(\mathbf{p},\omega_s) = [\mathbf{S}(\mathbf{p},\omega_s)]^{-1}\mathbf{f}(\omega_s) \tag{5}$$

$$\mathbf{S}(\mathbf{p},\omega_s) = \hat{\mathbf{K}}(\mathbf{p},\omega_s) - \omega^2\mathbf{M}(\omega_s) \tag{6}$$

in which $\mathbf{M}(\omega_s)$ is the mass matrix, and $\hat{\mathbf{K}}(\mathbf{p},\omega_s)$ is the complex stiffness matrix including the hysteretic damping effect represented as

$$\hat{\mathbf{K}}(\mathbf{p},\omega_s) = \overline{\mathbf{K}}(\omega_s) + \sum_{r=1}^{N_p} p_r \overline{\mathbf{K}}_r(\omega_s) \tag{7}$$

where $\overline{\mathbf{K}}$ is the stiffness matrix for the base case when p_r are zero, and $\overline{\mathbf{K}}_r$ denotes the stiffness matrix for the r-th region with the base value of $\overline{G}_r$. To identify the stiffness parameters minimizing the estimation error of the mathematical model in average sense, a constrained optimization problem is defined in this study as:

$$\min_{\mathbf{p}} J(\mathbf{p}) = \sum_{i=1}^{N_{mp}-1}\sum_{j=1}^{N_{mp}-i}\sum_{s=1}^{N_{fq}} \left(1 - \frac{y_{i+j}(\omega_s)}{y_i(\omega_s)} \cdot \frac{H_i(\mathbf{p},\omega_s)}{H_{i+j}(\mathbf{p},\omega_s)}\right)^T \mathbf{W} \left(1 - \frac{y_{i+j}{}^*(\omega_s)}{y_i{}^*(\omega_s)} \cdot \frac{H_i{}^*(\mathbf{p},\omega_s)}{H_{i+j}{}^*(\mathbf{p},\omega_s)}\right) \tag{8}$$

subject to the inequality constraints [2]:

$$G_{Backfill-1} \le G_{Backfill-2}, \quad G_{Gravel-2} \le G_{Gravel-1}, \quad G_{Gravel-1} \le G_{Gravel-4}, \quad G_{Sand-1} \le G_{Sand-2} \tag{9a,b,c,d}$$

and bounds on the parameters [2]:

$$G_{rl} \le G_r \le G_{ru} \quad (r = 1,2,\cdots,N_p) \tag{10}$$

where G_{rl} and G_{ru} are the lower and upper bounds for G_r respectively as shown in Table 2. In Equation (8), $y(\omega_s)$ is the measured frequency response; superscript * denotes the complex conjugate; N_{fq} is the number of sampling frequency used for the calculation of the error function; N_{mp}

is the number of the measured frequency response used for the construction of the error function; and **W** is a diagonal matrix containing weight factors. In this study, the weighting factors are taken as the inverses of the square of the response amplitudes at the resonant frequency so that all response components may be equally weighted. The present optimization problem with the inequality constraints can be solved using the constrained steepest descent method [2].

6. Results of Identification

Identification of the stiffness parameters is carried out for NS-horizontal directions using the earthquake records measured in the structure and free-field soil. The earthquake records measured on March 5, 1996 at Hualien LSST site are used for identification of the stiffness parameters. Because the maximum ground peak acceleration of the earthquake is only 0.01 g as shown Figure 4, influence of the nonlinear behavior of the soil-structure interaction system may be neglected.

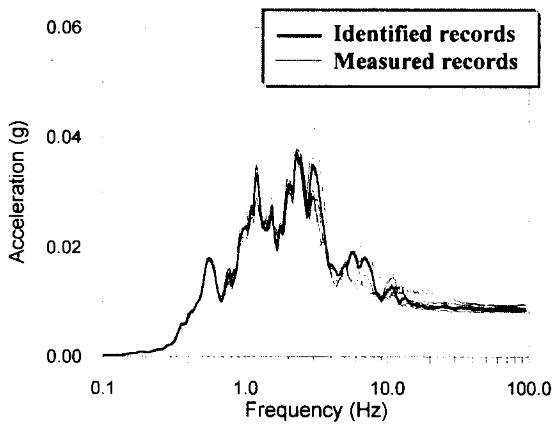

Figure 4 Measured and identified records

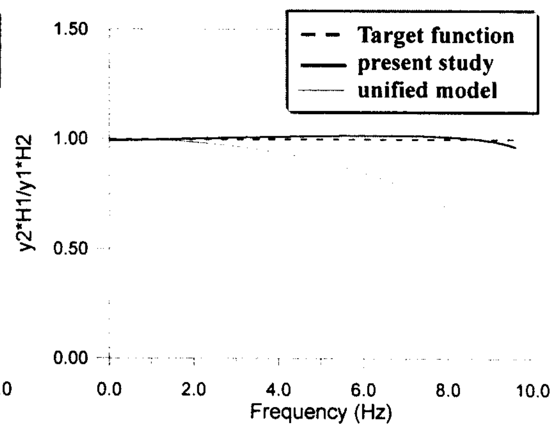

Figure 5 Error function for the identification

The error function for the parameter estimation is constructed using the earthquake response data measured at four points of the structure as shown Figure 2. It is found that the error function is calculated using the earthquake response data only as shown in Figure 5 and Equation (8). In this study, then, the smoothing technique by Parzen's spectral window is employed in order to carry out smoothing of the Fourier amplitude of measured response data. Almost four hundred frequency points are selected in the significant frequency range (2-10 Hz) for the Fourier amplitude of measured response data.

The properties of the unified model are used as the initial values for the identification. The constrained steepest descent method is employed to obtain the revised parameters. The final values after the 15th iteration are shown in Table 1 along with those of the unified model and FVT-correlated model [2]. Figure 6 shows the estimation error and convergence behaviors of the parameters during the iterations. The identified values are generally smaller than those of the unified model and very similar to the FVT-correlated model.

Figure 4 shows the response spectra of the identified input motion and records measured at the free field of Hualien site, which indicate that the responses are very similar to amplitude as well as frequency contents. On the other hand, the floor response spectra computed from the results of earthquake analysis using the identified parameters also agree very well with those from the observed responses, in contrast to those obtained using the unified model which are fairly off as shown in Figure 7 and 8. The results indicate that the identified parameters are very reasonable, suggesting that parameters can be accurately estimated with the earthquake response data only without using FVT.

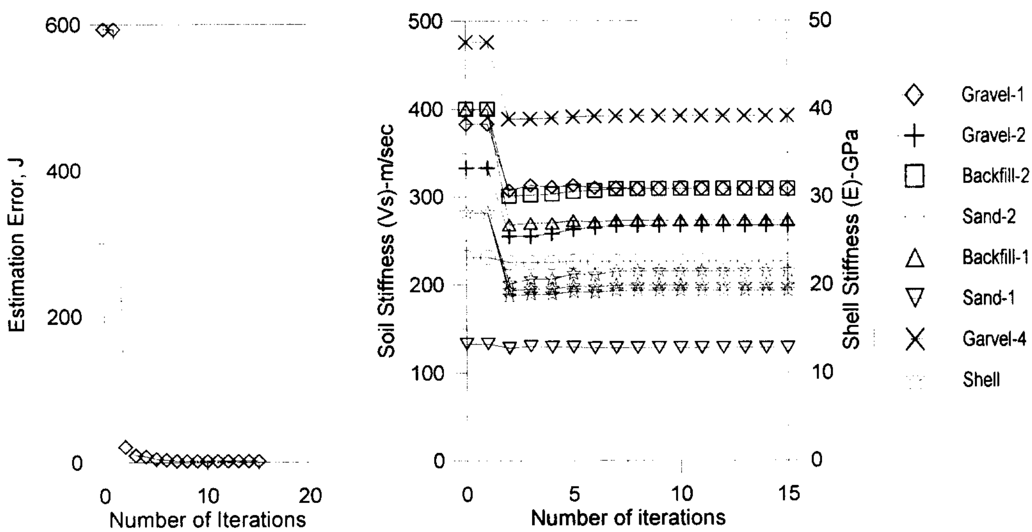

Figure 6 Transition of estimation error and convergence of unknown parameters

7. Conclusions

This study presents a new method to identify input motions and a finite element model for a SSI system using the earthquake response data. The simulated earthquake responses using the identified parameters and input motion for the Hualien soil-structure interaction system are shown to be in excellent agreement with the observed response data. It is expected that the proposed method can be effectively used in the identification of soil-structure interaction systems for which performing FVT is very difficult, if not impossible.

Acknowledgement

The authors would like to express their sincere appreciation for the financial supports from the Brain Korea 21 and also by the Korea Institute of Nuclear Safety (1993-1997).

References

1. Tang, H.T., Stepp, J.C., *et al*, 'The Hualien Large-Scale Seismic Test for the Soil-Structure Interaction Research,' *Proc. 11th SMiRT*, K1, pp. 69-74,1991.

2. Yun, C.B., Choi, J.S. and Kim, J.M., 'Identification of the Hualien Soil-Structure Interaction System', *Soil Dynamics and Earthquake Engineering*, 1999, **18** (6), 395-408.
3. Choi, J.S., Yun, C.B. and Kim, J.M., 'Earthquake response analysis of the Hualien large scale seismic test structure using updated soil-structure properties based on vibration test data.' *Earthquake Engineering and Structural Dynamics*, **30**, pp1-26, 2001.
4. CRIEPI. The Unified Model of the Ground for FVT-2 analysis. *Hualien LSST Meeting*, Taiwan, 1993.
5. Zhao, C. and Valliappan, S., 'An efficient wave input procedure for infinite media', *Communications in Numerical Methods in Engineering*, pp. 407-415, 1993.
6. Yun, C.B., Kim, J.M. and Hyun, C.H., 'Axisymmetric elastodynamic infinite elements for multi-layered half-space', *Int. J. Num. Meth. Engng.*, 1995, **38**, 3723-3743.

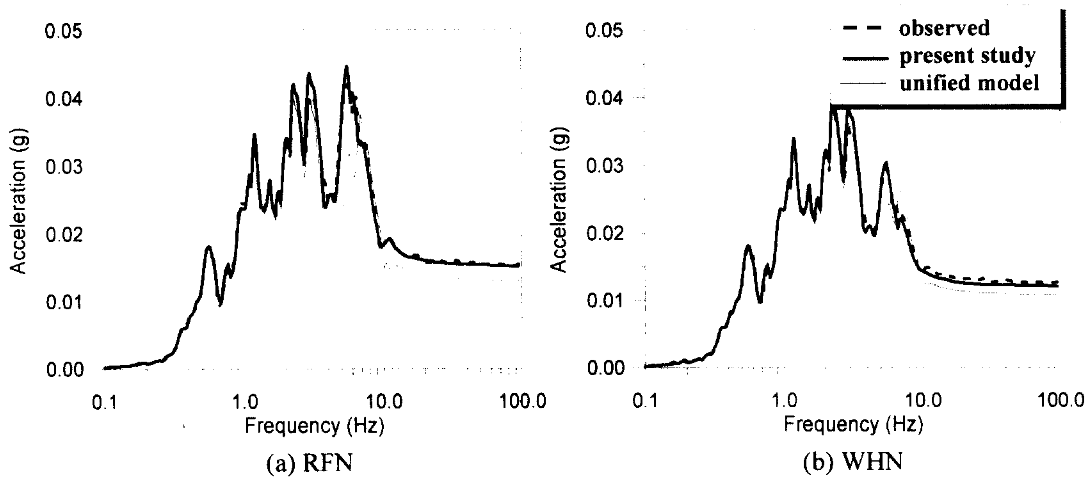

Figure 7 Response spectra obtained for NS-direction at Hualien LSST structure (5% Damping)

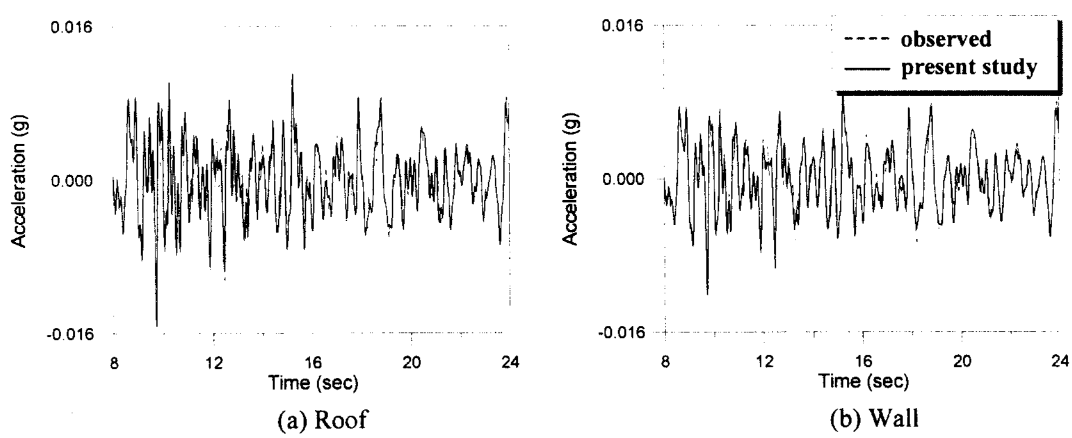

Figure 8 Time history obtained for NS-direction at Hualien LSST structure